

## Modeling flow instability of an Algerian sand with the dilatancy rule in CASM

Catarina Ramos <sup>\*1</sup>, António Viana da Fonseca <sup>1a</sup> and Jean Vaunat <sup>2b</sup>

<sup>1</sup> CONSTRUCT-GEO, Faculty of Engineering (FEUP), University of Porto, Portugal

<sup>2</sup> Departamento de Ingeniería del Terreno, Universitat Politècnica de Catalunya, Barcelona, Spain

(Received September 25, 2014, Revised October 14, 2015, Accepted October 23, 2015)

**Abstract.** The aim of the present work was the study of instability in a loose sand from *Les Dunes* beach in Ain Beninan, Algeria, where the Boumerdès earthquake occurred in 2003. This earthquake caused significant structural damages and claimed the lives of many people. Damages caused to infrastructures were strongly related to phenomena of liquefaction. The study was based on the results of two drained and six undrained triaxial tests over a local sand collected in a region where liquefaction occurred. All the tests hereby analyzed followed compression stress-paths in monotonic conditions and the specimens were isotropically consolidated, since the objective was to study the instability due to static loading as part of a more general project, which also included cyclic studies. The instability was modeled with the second-order work increment criterion. The definition of the instability line for *Les Dunes* sand and its relation with yield surfaces allowed the identification of the region of potential instability and helped in the evaluation of the susceptibility of soils to liquefy under undrained conditions and its modeling. The dilatancy rate was studied in the points where instability began. Some mixed tests were also simulated, starting with drained conditions and then changing to undrained conditions at different time steps.

**Keywords:** constitutive model; critical state; flow liquefaction; instability of sands

---

### 1. Introduction

Every day, geotechnical engineers have to deal with problems related to failure of granular soils. One of these problems is the liquefaction of loose to medium sands under undrained conditions, which can cause devastating damages. This is the case of tailing deposits of silty to sandy-silt materials (Bedin *et al.* 2012).

Constitutive models have been proposed to reproduce the response of soils to applied loads (Lade 1994, Dafalias and Manzari 2004, Andrade 2009 and Andrade *et al.* 2013). One of the widely used frameworks to formulate constitutive models is the elasto-plastic theory. Elasto-plastic models based on the critical state concept have been used to simulate real soil behaviour and its application on the modeling of sand have gained acceptance in the geotechnical engineering community (Taiebat and Dafalias 2008 and Wang *et al.* 2002). Some examples are the

---

\*Corresponding author, M.Sc., E-mail: [catarinacorreiramos@gmail.com](mailto:catarinacorreiramos@gmail.com)

<sup>a</sup> Ph.D., E-mail: [viana@fe.up.pt](mailto:viana@fe.up.pt)

<sup>b</sup> Ph.D., E-mail: [jean.vaunat@upc.edu](mailto:jean.vaunat@upc.edu)

Cam-clay model (Roscoe *et al.* 1958), the modified Cam-clay model (Roscoe and Burland 1968) and the Clay and Sand model (Yu 1998), among others (Zouain *et al.* 2010, González 2011). To better simulate sand behaviour, a “state parameter” was introduced and is defined as the difference between specific volume (or void ratio) and the specific volume (or void ratio) at the critical state at the same mean effective stress (Been and Jefferies 1985).

The study of instability is a huge concern when dealing with the safety of dams, structures, excavations or slopes because instability eventually leads to failure. The state of instability in soils can lead to flow liquefaction (Andrade 2013). Several studies and laboratory tests were done over the years to evaluate the soil susceptibility to instability and static liquefaction (Lade 1992, 1994, Lade *et al.* 2009, Ramos 2010 and Lade and Yamamuro 2011). Many authors have developed studies on flow liquefaction, particularly static liquefaction (Borja 2006, Andrade 2009, Soares *et al.* 2011, Bedin *et al.* 2012, Andrade *et al.* 2013 and Schnaid *et al.* 2013). In this work, the instability that leads to flow liquefaction under undrained conditions is studied according to the second-order work increment criterion. This work complements the studies that have been done in a particular sand, from *Les Dunes* beach in Ain Benian in Algeria, where in 2003 the Boumerdès earthquake occurred, which caused many cyclic liquefaction related occurrences, which are described in Viana da Fonseca and Soares (2014).

## 2. CASM model

In this section, the Clay and Sand Model (CASM), which is used to simulate the behaviour of *Les Dunes* sand in this work, is briefly described (Yu 1998). It is a unified critical state constitutive model and it is based on the state parameter.

CASM assumes the same elastic behaviour as the standard Cam-clay models, being the bulk and shear moduli defined by

$$K = \frac{\nu \times p'}{\kappa} \quad \text{and} \quad G = \frac{3 \times (1 - 2\nu)}{2 \times (1 + \nu)} K \quad (1)$$

In this section, the Clay and Sand Model (CASM), which is used to simulate the behaviour of *Les Dunes* sand in this work, is briefly described (Yu 1998). It is a unified critical state constitutive model and it is based on the state parameter.

CASM assumes the same elastic behaviour as the standard Cam-clay models, being the bulk and shear moduli defined by

$$F = \left( \frac{q}{Mp'} \right)^n + \ln \left( \frac{p'}{p'_o} \right) \frac{1}{\ln r} \quad (2)$$

In this section, the Clay and Sand Model (CASM), which is used to simulate the behaviour of *Les Dunes* sand in this work, is briefly described (Yu 1998). It is a unified critical state constitutive model and it is based on the state parameter.

CASM assumes the same elastic behaviour as the standard Cam-clay models, being the bulk and shear moduli defined by

$$d = \frac{\delta \varepsilon_p^p}{\delta \varepsilon_q^p} = \frac{9(M - \eta)}{9 + 3M - 2M\eta} \quad (3)$$

where  $\eta = q/p'$  and  $\eta$  is the critical state failure ratio.

The plastic potential is obtained by the integration of Rowe's stress dilatancy relation and is defined by

$$g(p', q, \beta) = 3M \ln \frac{p'}{\beta} + (3 + 2M) \ln \left( \frac{2q}{p'} + 3 \right) - (3 - M) \ln \left( 3 - \frac{q}{p'} \right) = 0 \quad (4)$$

where  $\eta = q/p'$  and  $\eta$  is the critical state failure ratio.

The plastic potential is obtained by the integration of Rowe's stress dilatancy relation and is defined by

$$dp'_0 = \frac{(1+e)p'_0}{\lambda - \kappa} d\varepsilon_p^p \quad (5)$$

### 3. Instability criterion

One of the criteria for detecting the onset of instability in geomechanical systems is based on the second-order work. Hill (1958) was the first to propose this instability criterion and Bazant and Cedolin (1991) presented a demonstration based on the laws of thermodynamics to prove it. When the second-order work increment is zero instability can occur in the soil and the stress-path falls in the region of potential instability. In a triaxial test axisymmetric conditions, the second-order work is defined by

$$d^2W = dp' d\varepsilon_v + dq d\varepsilon_s \quad (6)$$

One of the criteria for detecting the onset of instability in geomechanical systems is based on the second-order work. Hill (1958) was the first to propose this instability criterion and Bazant and Cedolin (1991) presented a demonstration based on the laws of thermodynamics to prove it. When the second-order work increment is zero instability can occur in the soil and the stress-path falls in the region of potential instability. In a triaxial test axisymmetric conditions, the second-order work is defined by

### 4. Numerical simulations

Pinheiro (2009) and Rocha (2010) developed a series of triaxial tests (two under drained and six under undrained conditions) with different initial confining pressures on *Les Dunes* sand.

CASM is implemented in *Code\_Bright* (Olivella and Vaunat 2006), the code used to obtain the numerical solutions of these triaxial tests. The classical critical state parameters ( $\kappa$ ,  $\lambda$  and  $M$ ) and additionally the Poisson's ratio, were defined from the undrained and drained tests, being reported in Viana da Fonseca and Soares (2012). The other two parameters had to be defined in a fitting process using the results of the same tests as detailed in Ramos (2013). This is illustrated in Fig. 1. The model parameters that characterize *Les Dunes* sand are resumed in Table 1.

Figs. 2 and 3 represent, respectively, the deviatoric stress and pore pressure versus the axial strain curves and the stress-paths for the undrained tests performed in the laboratory together with the respective simulation with this model. The numerical and the experimental results are very similar, evidencing clearly the high performance of CASM as implemented in *Code\_Bright* to simulate the behavior of *Les Dunes* sand up to the instability point.

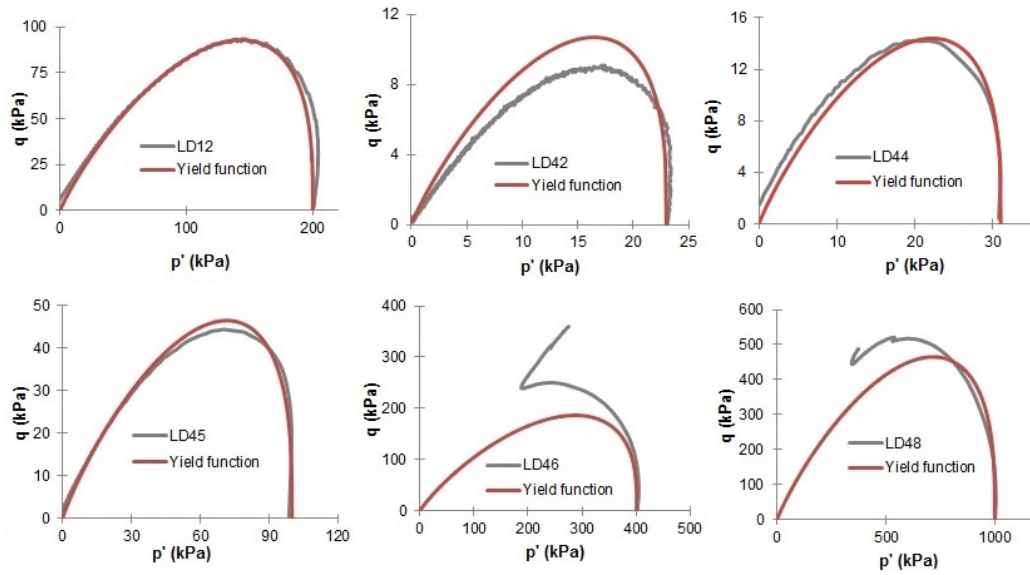


Fig. 1 Yield surfaces for undrained triaxial tests

Table 1 Material parameters

Parameters	Value
Poisson's ratio, $\nu$	0.362
Slope of the isotropic swelling line (in $v-\ln p'$ space), $\kappa$	$5.0 \times 10^{-3}$
Slope of Critical State Line (in $v-\ln p'$ space), $\lambda$	0.021
Spacing ratio, $r$	15
Shape parameter, $n$	3
Critical state parameter, $M$	1.3047

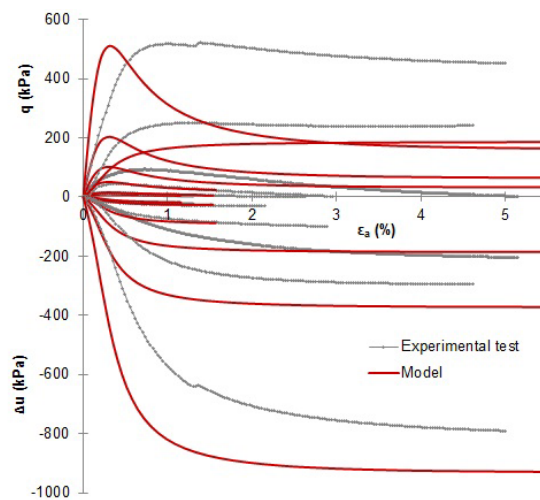


Fig. 2 Deviatoric stress and pore pressure *versus* axial strain for undrained tests

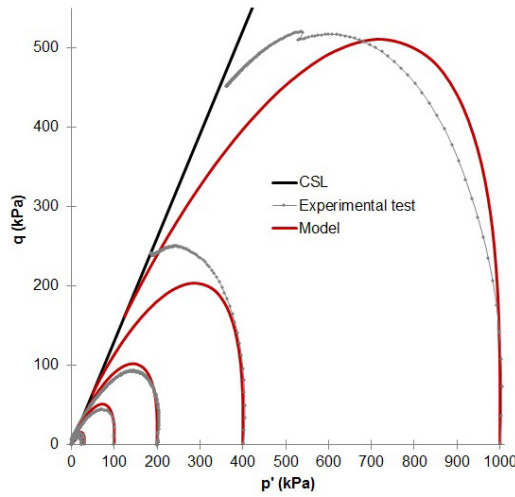


Fig. 3 Stress-path for undrained tests

## 5. Instability of Les Dunes sand

### 5.1 Instability line of Les Dunes sand

The location of the instability line is defined by the values corresponding to the peak in the deviatoric stress, i.e., the top of the current yield surfaces (Lade and Yamamuro 2011), using the undrained tests results provided by the program (Fig. 4). According to Lade (1994), for materials isotropically consolidated under undrained conditions, the top of the yield surface is the onset of flow liquefaction.

### 5.2 Drained test results and instability line

According to Lade and Yamamuro (2011), a soil will remain stable inside the region of potential instability if it is drained. Fig. 5 shows the simulation of the two drained tests in  $p'$ - $q$  space. The stress-paths overpass the instability line and do not change their paths, consequently

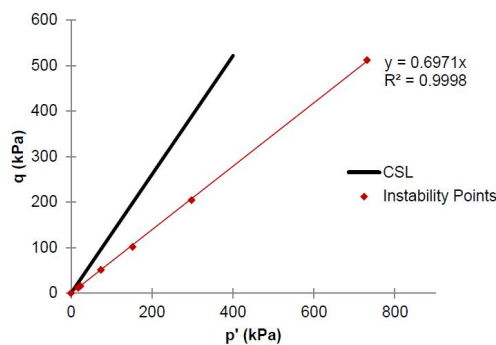


Fig. 4 Definition of the instability line

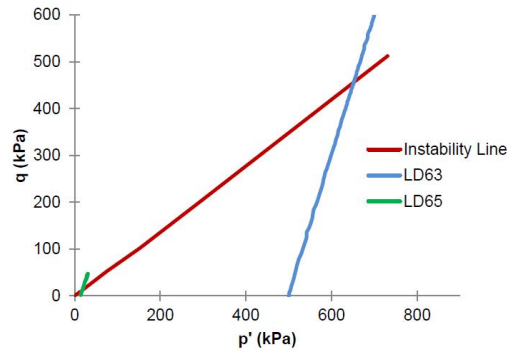


Fig. 5 Stress-path of drained tests and instability line

they stay stable. The number of drained triaxial tests is not enough to be absolutely conclusive, but it can be assumed that in principle for triaxial tests in drained conditions in this state ( $e$  and  $p'_0$ ) instability does not occur.

### 5.3 Simulation of drained-undrained tests

A simulation of a singular test, where a specimen was first submitted to drained condition and then, at an intermediate loading level, the condition changed to undrained, i.e., the water flux in the specimen stops, was conducted to evaluate the sensibility of this model to detect the triggering of instability. In Fig. 6 the stress-paths for several simulations are represented. In each, the drained process was stopped at different times. The Critical State Line and the Instability Line are also represented, with the intention of being reference lines. The stress-path for 250 hours represents the fully drained test. All tests performed follow the drained path until the moment they start to be undrained.

For tests that start to be undrained after their stress-path passes the instability line, the moment they are under undrained conditions they are already instable. If a test starts to be undrained before reaching the instability line, it follows a typical undrained stress-path, with increase of the

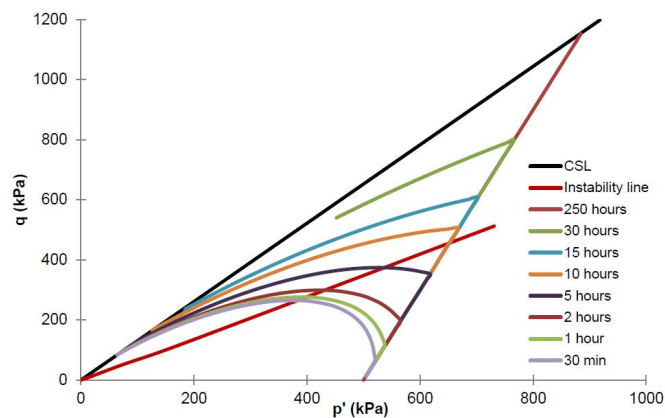


Fig. 6 Stress-paths of drained-undrained simulations

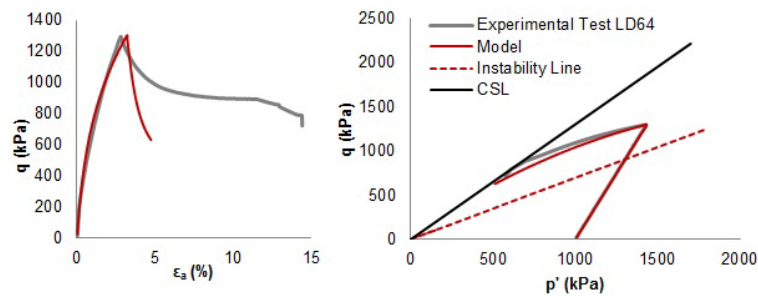


Fig. 7 Stress-strain curves and stress-path of LD64 test

deviatoric stress while the effective mean stress decreases. The moment it reaches that instability line, the deviatoric stress begins to reduce. The peak of the deviatoric stress is really close to that point where the stress-path crosses the instability line, so it can be concluded that if a test changes from drained to undrained conditions before its path reaches the instability line, it stays stable. When the two curves intersect on the undrained path, the specimen becomes unstable and the deviatoric stress starts decreases.

As the drained to undrained process occurs at different steps, at different deviatoric stresses, the  $p'_0$  value for each simulation is obviously different and so the final point of each stress-path is different.

The behaviour plotted in Fig. 6 is due only to a specific state parameter corresponding to a singular void ratio and effective stress. Similar behaviour will be expected although with distinct position of the critical state, for other state parameters. This will be a subject to develop in the future, recognizing that, in a 3 dimensional space of  $e$ - $p'$ - $q$ , an instability surface is expected (Lade and Yamamuro 2011).

In purely drained conditions and with controlled trajectories, as the ones treated, true liquefaction is not observed. However the authors admit that partial instability can occur, as a result of a decrease in total confining pressure or an increase in pore pressure caused by injection of water into the soil element (Lade 1994), where the conditions are different.

An experimental triaxial test (LD64) that started to be performed under drained conditions but at a certain point, the BP valves had to be closed and the test became undrained, was performed. The test was simulated using the model presented in this paper, to study the response of the code to this test and validate the simulations aforementioned. A comparison between the experimental data and the simulations is presented in Fig. 7, showing both stress-strain curves and stress-path similar and the good adaption of the model to the real experimental results. When the test changes from drained to undrained conditions, the deviatoric stress decreases but the plastic strain does not stop. Softening is observed and the soil deforms plastically with decreasing levels.

Also in Fig. 7, the stress-path is represented with the critical state line and the instability line defined for this sand. It is observed that when the test becomes undrained, the stress-path is already inside the region of potential instability. After that point, both the deviatoric and effective mean stresses decrease due to the instable prior unstable condition.

## 6. Dilatancy rate

According to Rowe (1962), dilatancy and strength of a group of particles in contact when

Table 2 Dilatancy rate for undrained tests at the instability line

Triaxial Test	$q$ (kPa)	$p'$ (kPa)	$\eta = q/p'$	$d$
LD12	102	152	0.666	0.514
LD42	12	18	0.647	0.528
LD44	16	23	0.664	0.516
LD45	51	74	0.691	0.497
LD46	204	298	0.685	0.501
LD48	512	731	0.701	0.490

Table 3 Dilatancy rate for the intersection point of the stress-path with the instability line

Triaxial Test	$q$ (kPa)	$p'$ (kPa)	$\eta$	$d$
LD63	454	652	0.697	0.493
LD65	14	20	0.697	0.493

subjected to a deviatoric stress system depend on three main parameters: the friction angle between the surface of the particles, the geometrical angle of packing and the degree of energy loss during remolding. For each undrained test, Eq. (3) was applied, using the deviatoric and effective mean stress values corresponding to the instability point (Table 2).

Analyzing the values of the dilatancy rate obtained on each undrained test, it can be concluded that the value of dilatancy for *Les Dunes* sand at the instability point is about 0.5. That means that when the dilatancy rate reaches the value of 0.5, the soil may experience instability.

Drained tests remain stable after their stress-path crosses the instability line. The dilatancy rate in the intersection point of the instability line and the drained test stress-path was studied.

The instability line appears to be both related to a constant value of dilatancy (0.493) or a constant value of stress ratio (0.697). According to instability concept, it is the direction of plastic strain that initiate the instability and thus it is more rational to link the instability line to the value of dilatancy. However, as in CASM model the dilatancy depends only on the stress ratio ( $\eta$ ), both concepts are equivalent. A conclusion of that is that the shape of the instability line in  $p'$ - $q$  diagram (straight line) validates the assumption made for the dilatancy rule in CASM model. The model appears then to allow for modeling liquefaction in materials where instability line is a straight line in the  $p'$ - $q$  space.

## 7. Second order work

In order to validate the described trends and to continue the study of instability in *Les Dunes* sand, the second-order work criterion was applied to the tests. Using the expression of Eq. (6) the second-order work increment was calculated for each step of the simulation.

### 7.1 Drained tests

The second-order work increment values were compared with the evolution of the axial strain for the drained tests (Fig. 8). These results confirm what was defended above, for drained tests the

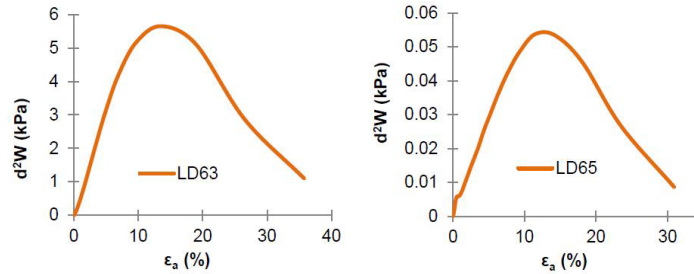


Fig. 8 Second-order work increment *versus* axial strain for drained tests

second-order work increment is always positive so they are stable.

### 7.2 Undrained tests

The same procedure was applied to the undrained test results. In this case, the deviatoric stress was also represented, to show that when the second-order work increment is zero (starting to be negative) the deviatoric stress reaches a peak (Fig. 9). It can be concluded that when the second-order work increment is zero and begins to be negative, the deviatoric stress is maximum (and starts decreasing). This confirms the instability criterion explained above.

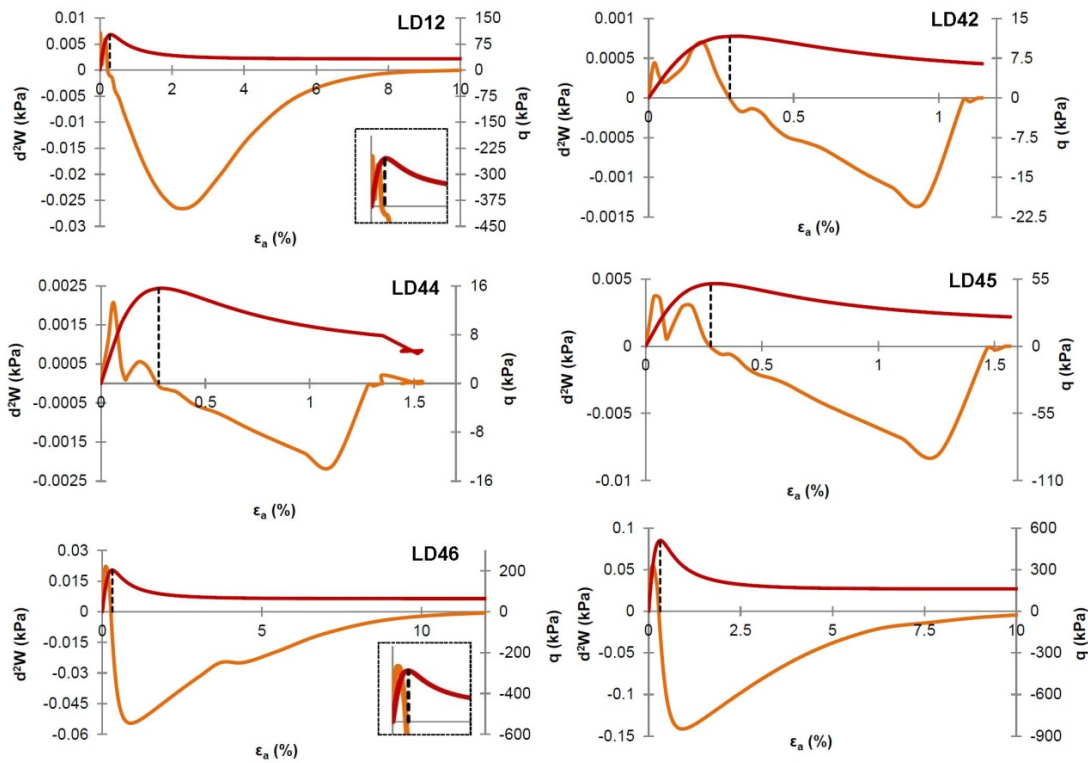


Fig. 9 Second-order work increment and deviatoric stress *versus* axial strain for undrained tests

### 7.3 Drained-undrained tests

It is also important to study the second-order work increment in the mixed tests simulated. Fig. 10 shows the evolution of  $d^2W$  and the deviatoric stress with the time steps (in hours). In this analysis the horizontal axis was chosen to be the time instead of the axial strain, in order to evaluate what happens in the time step when the conditions change from drained to undrained. Some conclusions can be made regarding these results.

First, for the tests that overpass the instability line under drained conditions and only after that turned to undrained conditions (30 h, 15 h and 10 h), the second-order work increment is zero in the exact time when the test starts to be undrained. This is justified by the fact that the stress-path is inside the region for potential instability so, when the conditions change to undrained the peak of the deviatoric stress is by definition this same value of  $q$  and it starts to drop. As for the tests

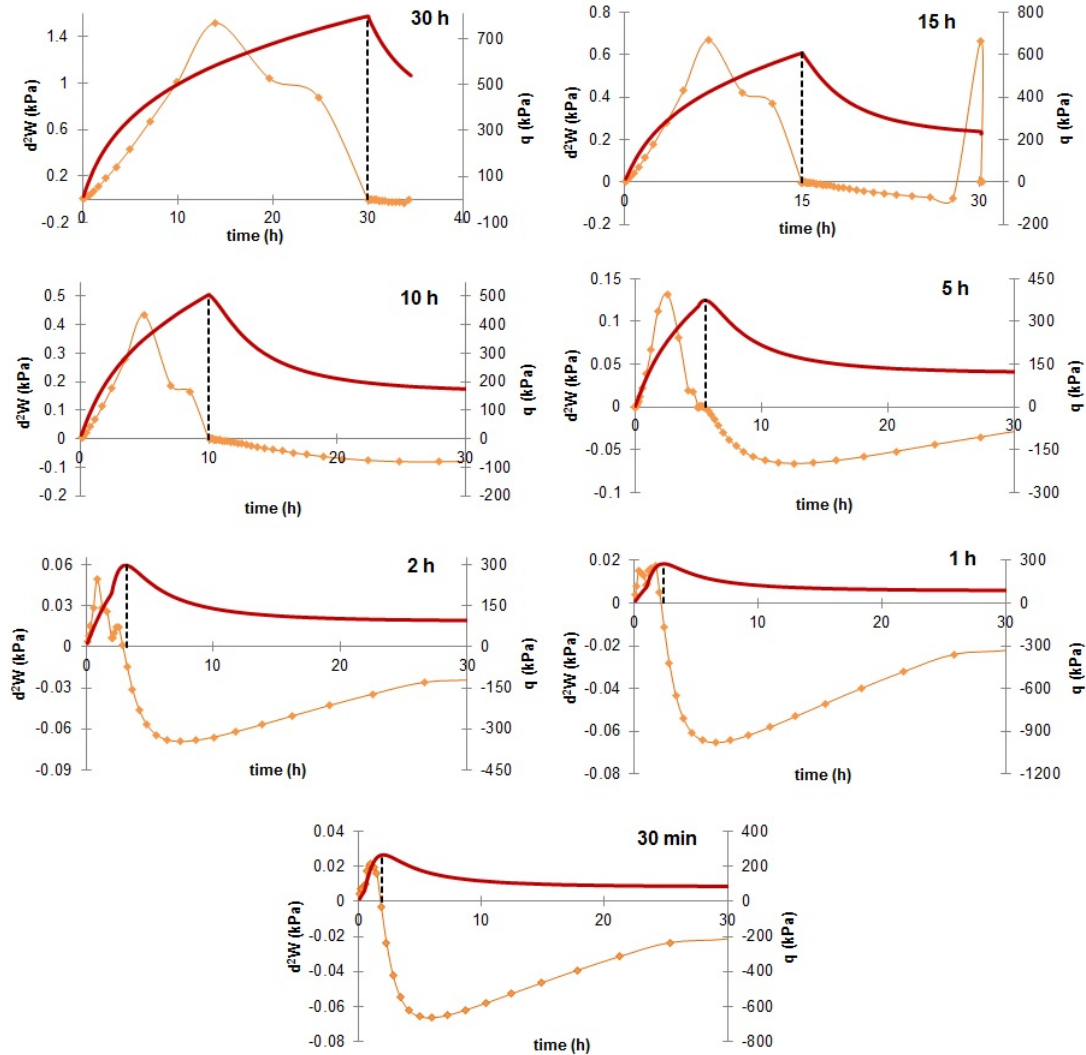


Fig. 10 Second-order work increment and deviatoric stress *versus* axial strain for mixed tests

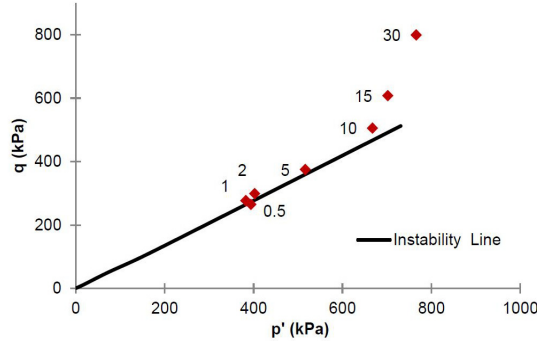


Fig. 11 Instability points for each test

that change to undrained conditions while the stress-path lies under the instability line (5 h, 2 h, 1 h and 30 min), they stay stable until crossing that line.

The peak of the deviatoric stress is reached when the stress-path crosses the instability line, in a time step after the time when undrained conditions start (Fig. 11).

## 8. Definition of CSL, NCL and instability line in $e$ - $\ln p'$ space

In this section, the Critical State Line, the Normal Compression Line and the Instability Line are defined in  $e$ - $\ln p'$  space and the differences between them are evaluated.

The equation of the CSL is defined with the results of some drained and undrained tests performed in *Les Dunes* sand (Eq. (7)).

$$e = -0.021 \ln p' + 0.9659 \quad (7)$$

The NCL is defined by the values of  $p'_0$ , the first point of the stress-path and it is parallel to the CSL. To define its equation, the value of  $p'$  in Eq. (7) has to be replaced by a value related with  $p'_0$ . To determine this value, the expression of the yield surface was equated to the expression of the CSL in the Critical State Theory, as it is shown in the Eq. (8).

$$Mp' = Mp' \left( \ln \left( \frac{p'_0}{p'} \right) \frac{1}{\ln r} \right)^{\frac{1}{n}} \Leftrightarrow p' = \frac{p'_0}{r} \quad (8)$$

Replacing the value of  $p'$  in Eq. (7), the NCL is defined in  $e$ - $\ln p'$  space by Eq. (9).

$$e = -0.021 \ln p'_0 + (0.021 \ln r + 0.9659) \quad (9)$$

To define the instability line, the yield function is equated and the result is an expression that relates  $\ln p'$  with a function containing  $p'_0$  (Eq. (10)).

$$0.6971 p' = Mp' \left( \ln \left( \frac{p'_0}{p'} \right) \frac{1}{\ln r} \right)^{\frac{1}{n}} \Leftrightarrow \ln p' = \ln p'_0 - \left( \frac{0.6971}{M} \right)^n \ln r \quad (10)$$

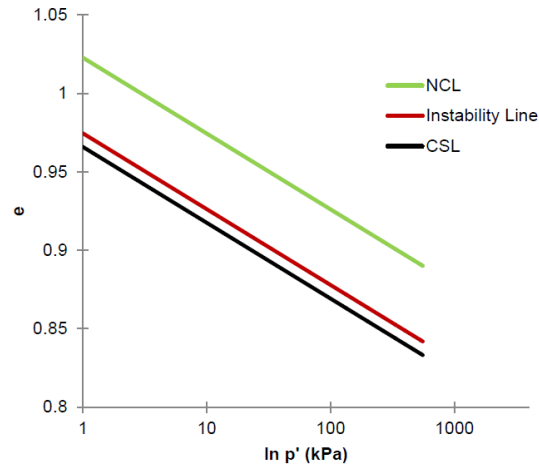


Fig. 12 CSL, NCL and Instability line in  $e$ -  $\ln p'$  space

Replacing the value of  $p'$  in Eq. (7), the instability line is defined in  $e$ - $\ln p'$  space as follows

$$e = -0.021 \ln p'_0 + 0.021 \left( \frac{0.6971}{M} \right)^n \ln r + 0.9659 \quad (11)$$

In Fig. 12 the three lines are represented. The parameters of the sand were replaced in the expressions above. It can be concluded that the instability line is also parallel to the CSL and NCL and it is situated between them. The instability line is closer to the CSL than to the NCL.

## 9. Conclusions

In this study the definition of the instability line for *Les Dunes* sand and its relation with yield surfaces allowed to prove that:

- The instability line in this sand is a straight line, passing in the peak of the deviatoric stress in  $q$ - $p'$  space, for the undrained tests.
- According to this criterion, a specimen under drained conditions is never unstable.
- A specimen loaded in undrained conditions may become unstable after its stress-path crosses the instability line and enters the region of potential instability.
- This pattern of instability was also confirmed in the simulation of drained-undrained tests, these tests starting to be drained and at different times the conditions were changed to undrained.
- If the undrained conditions start when the stress-path has already cross the instability line, the specimen may already be unstable (second order work increment is zero in that point), while, if a test starts to be undrained before reaching the instability line, it stays stable.
- Only when the undrained stress-path crosses the instability line, that is when the second order work increment is zero, instability may occur.
- As for the dilatancy rate, proposed by Rowe (1962), it was proven to be around 0.49 in the point where the stress-paths intersect the instability line.

- So, it is the authors believing that, since in CASM model, the dilatancy depends on the stress ratio, which controls the dilatancy rate:
- The value of the stress ratio is the slope of the instability line.
- The shape of the instability line in  $p'$ - $q$  diagram (straight line) validates the assumption made for the dilatancy rule in CASM model.

The results found can lead to a better understanding and modeling of instabilities in saturated granular soils, allowing to a good prediction of soil susceptibility for liquefaction triggering.

## References

- Andrade, J.E. (2009), "A predictive framework for liquefaction instability", *Géotechnique*, **59**(8), 673-682.
- Andrade, J.E., Ramos, A.M. and Lizcano, A. (2013), "Criterion for flow liquefaction instability", *Acta Geotechnica*, **8**(5), 525-535
- Arroyo, M., Amaral, M.F., Romero, E. and Viana da Fonseca, A. (2013), "Isotropic yielding of unsaturated cemented silty sand", *Can. Geotech. J.*, **50**(8), 807-819.
- Bazant, Z. and Cedolin, L. (1991), *Stability of Structures. Elastic, Inelastic, Fracture and Damage Theories*, Dover Publications, Mineola, NY, USA.
- Bedin, J., Schnaid, F., Viana da Fonseca, A. and Costa-Filho, L. (2012), "Gold tailings liquefaction using critical state soil mechanics concepts", *Géotechnique (ICE)*, **62**(3), 263-267.
- Been, K. and Jefferies, M.G. (1985), "A state parameter for sands", *Géotechnique*, **35**(2), 99-112.
- Borja, R.I. (2006), "Condition for liquefaction instability in fluid saturated granular soils", *Acta Geotechnica*, **1**(4), 211-224.
- Coussy, O., Pereira, J.M. and Vaunat, J. (2010), "Revisiting the thermodynamics of hardening plasticity for unsaturated soils", *Comput. Geotech.*, **37**(1), 207-215.
- Dafalias, Y.F. and Manzari, M.T. (2004), "Simple plasticity sand model accounting for fabric change effects", *J. Eng. Mech.*, **130**(6), 622-633.
- González, N.A. (2011), "Development of a family of constitutive models for Geotechnical applications", Ph.D. Dissertation; UPC, Barcelona, Spain.
- Hill, R. (1958), "A general theory of uniqueness and stability in elastic-plastic solids", *J. Mech, Phys. Solids*, **6**(3), 236-249.
- Jeremic, B., Cheng, Z., Taiebat, M. and Dafalias, Y. (2008), "Numerical simulation of fully saturated porous material", *Int. J. Numer. Anal. Meth. Eng.*, **32**(13), 1635-1660.
- Kim, M.K. and Lade, P.V. (1988), "Single hardening constitutive model for frictional materials, I. Plastic potential function", *Comput. Geotech.*, **5**(4), 307-324.
- Lade, P.V. (1992), "Static instability and liquefaction of loose fine sandy slopes", *J. Geotech. Eng.*, **118**(1), 51-71.
- Lade, P.V. (1994), "Instability and liquefaction of granular materials", *Comput. Geotech.*, **16**(2), 123-151.
- Lade, P.V. and Yamamuro, J.A. (2011), "Evaluation of static liquefaction potential of silty sand slopes", *Can. Geotech. J.*, **48**(2), 247-264.
- Lade, P.V., Yamamuro, J.A. and Liggio, C.D. Jr. (2009), "Effects of fines content on void ratio, compressibility and static liquefaction of silty sand", *Geomech. Eng., Int. J.*, **1**(1), 1-15.
- Manzari, M.T., Dafalias, Y.F. (1997), "A critical state two-surface plasticity model for sands", *Géotechnique*, **47**(2), 255-272.
- Olivella, S. and Vaunat, J. (2006), "Application of Code\_Bright\_GiD to geotechnical problems", *Proceedings of the 3rd GiD Conference*, Barcelona, Spain, March, p.10.
- Pinheiro, A. (2009), "Laboratory evaluation of the status conditions that led to phenomena of liquefaction of dune sands in the 2003 earthquake in Boumerdès", Master Thesis; FEUP, Porto, Portugal. [In Portuguese]
- Pinyol, N., Vaunat, J. and Alonso, E.E. (2007), "A constitutive model for soft clayey rocks that include weathering effect", *Géotechnique*, **57**(2), 137-151.

- Ramos, A.M. (2010), "Instability in Sands", Ph.D. Dissertation; Faculty of Engineering Universidad de los Andes, Bogotá, Colombia.
- Ramos, C. (2013), "Modelling sand instability within the framework of critical state soil mechanics", Master Thesis; FEUP, Porto, Portugal.
- Rios, S., Viana da Fonseca, A. and Baudet, B.A. (2012), "The effect of the porosity/cement ratio on the compression of cemented soil", *J. Geotech. Geoenviron. Eng.*, **138**(11), 1422-1426.
- Rios, S., Viana da Fonseca, A. and Baudet, B.A. (2013), "On the shearing behaviour of an artificially cemented soil", *Acta Geotechnica*, **9**(2), 215-226. DOI: 10.1007/s11440-013-0242-7
- Rocha, J. (2010), "Definition of liquefaction in triaxial conditions in the light of the theory of critical states and assessment of risk by reason of seismic waves velocities on a dune sand", Master Thesis; FEUP, Porto, Portugal. [In Portuguese]
- Roscoe, K.H. and Burland, J.B. (1968), "On the generalized stress-strain behaviour of wet clay", *Eng. Plast.*, 535-609.
- Roscoe, K.H., Schofield, A.N. and Wroth, C.P. (1958), "On the yielding of soils", *Géotechnique*, **8**(1), 22-53.
- Rowe, P.W. (1962), "The stress-dilatancy relation for static equilibrium of an assembly of particles in contact", *Proc. Roy. Soc.*, **269**(1339), 500-527.
- Sadrekarami, A. and Olson, S.M. (2011), "Yield strength ratios, critical strength ratios, and brittleness of sandy soils from laboratory tests", *Can. Geotech. J.*, **48**(3), 493-510.
- Schnaid, F., Bedin, J., da Fonseca, A. and Filho, L. (2013), "Stiffness and strength governing the static liquefaction of tailings", *J. Geotech. Geoenviron. Eng.*, **139**(12), 2136-2144.
- Soares, M., Bedin, J., Silva, J. and Viana da Fonseca, A. (2011), "Monotonic and cyclic liquefaction assessment on silty soils by triaxial tests with bender elements", *Proceedings of International Conference in Advances in Geotechnical Engineering*, Perth, Australia, November, Volume 1, pp. 819-826.  
[www.icage2011.com.au](http://www.icage2011.com.au)
- Taiebat, M. and Dafalias, Y.F. (2008), "SANISAND: simple anisotropic sand plasticity model", *Int. J. Numer. Anal. Meth. Geomech.*, **32**(8), 915-948.
- Viana da Fonseca, A. and Soares, M. (2012), "Effect of principal stress rotation on cyclic liquefaction", *Proceedings of the Second International Conference on Performance-Based Design in Earthquake Geotechnical Engineering*, Taormina, Italy, May, pp. 28-30.  
<http://www.2pbd-taormina.org> (Online)
- Viana da Fonseca, A. and Soares, S.M. (2014), "Effect of confinement pressure and inversion or principal stress rotation on cyclic behaviour of a sand liquefied during 2003 Boumerdès earthquake", *Bullet. Earthq. Eng. (BEEE)*, submitted.
- Wang, Z.L., Dafalias, Y.F., Li, X.S. and Makdisi, F.I. (2002), "State pressure index for modeling sand behaviour", *J. Geotech Geoenviron. Eng.*, **128**(6), 511-519.
- Yamamuro, J.A., Wood, F.M. and Lade, P.V. (2008), "Effect of depositional method on the microstructure of silty sand", *Can. Geotech. J.*, **45**(11), 1538-1555. DOI: 10.1139/T08-080
- Yu, H.S. (1998), "CASM: A unified state parameter model for clay and sand", *Int. J. Numer. Anal. Method. Geomech.*, **22**(8), 621-653.
- Zouain, N., Pontes-Filho, I. and Vaunat, J. (2010), "Potentials for the modified Cam-Clay model", *Eur. J. Mech. A/ Solids*, **29**(3), 327-336.